Day/night whole sky imagers for 24-h cloud and sky assessment: history and overview

Janet E. Shields,[1,*] Monette E. Karr,[1] Richard W. Johnson,[1] and Art R. Burden[2]

[1]Marine Physical Laboratory, Scripps Institution of Oceanography, University of California San Diego, 9500 Gilman Dr., La Jolla, California 92093-0701, USA

[2]Cooperative Institute for Climate and Satellites—NC, NOAA's National Climatic Data Center, 151 Patton Avenue, Asheville, North Carolina 28801-5001, USA

*Corresponding author: jshields@ucsd.edu

Received 7 December 2012; accepted 10 January 2013;
posted 29 January 2013 (Doc. ID 181371); published 6 March 2013

A family of fully automated digital whole sky imagers (WSIs) has been developed at the Marine Physical Laboratory over many years, for a variety of research and military applications. The most advanced of these, the day/night whole sky imagers (D/N WSIs), acquire digital imagery of the full sky down to the horizon under all conditions from full sunlight to starlight. Cloud algorithms process the imagery to automatically detect the locations of cloud for both day and night. The instruments can provide absolute radiance distribution over the full radiance range from starlight through daylight. The WSIs were fielded in 1984, followed by the D/N WSIs in 1992. These many years of experience and development have resulted in very capable instruments and algorithms that remain unique. This article discusses the history of the development of the D/N WSIs, system design, algorithms, and data products. The paper cites many reports with more detailed technical documentation. Further details of calibration, day and night algorithms, and cloud free line-of-sight results will be discussed in future articles.

OCIS codes: 010.0010, 010.1320, 010.1615, 110.4234, 120.0280, 290.1090.

1. Introduction

A family of fully automated digital whole sky imagers (WSIs) has been developed over the last three decades at the Atmospheric Optics Group (AOG), Marine Physical Laboratory (MPL), Scripps Institution of Oceanography (SIO), at the University of California San Diego [1,2–7]. These imagers are ground-based sensors that acquire digital imagery of the full sky down to the horizon in several spectral bands, in order to detect the presence and distribution of clouds. This development culminated in the day/night whole sky imagers (D/N WSIs) that automatically acquire high-quality digital imagery of the sky under all conditions, including full sunlight through moonlight and starlight conditions. The first of the WSIs was fielded in 1984 [4], followed by the D/N WSIs in 1992 [8–10]. The digital images, when combined with appropriate algorithms, provide assessment of cloud amount and location within the scene. The original day WSIs provided cloud assessment during the daytime [3]. The D/N WSIs also provide cloud assessment at night [7]. A sunset algorithm, although feasible, was not completed. The D/N WSIs can also be used to provide absolute radiance distribution and related atmospheric parameters. They distinguish between optically thin and opaque clouds in both day and night imagery, and at night they also provide cloud optical depth.

The WSIs were initially developed in support of research into cloud free line of sight (CFLOS) statistics and their impact on ground-based laser weapon applications [11,12]. Previous studies used models based on quite old CFLOS data and models based on satellite data [e.g., 13,14]. Each of these approaches

1559-128X/13/081605-12$15.00/0

had limitations. For example, the model based on satellite data was limited because a directional line of sight from a ground-based site is required, and this information normally cannot readily be obtained from satellite data due to the acquisition angles. Due to the different geometry, satellites do not provide cloud distribution within the hemispherical field of view of a ground-based radiation sensor.

As the systems continued in development, many more applications evolved. These have included: support of military test sites and satellite tracking stations [15,16]; experiments related to studies of laser communication [6,7]; support of global climate research [17]; research related to the impact of ozone on the ultraviolet (UV) radiation [5,18–20]; studies of ceilometer accuracy; and determination of CFLOS statistics for airborne laser applications and other applications [21,22]. For some of these applications, data were processed in archival mode, and in other cases the algorithms provided results in real time.

Since at least the mid-to-late 1990s, several groups have developed multispectral digital sky imagers for a variety of uses. An example of a day imager is the total sky imager (TSI) [23,24] using a silvered mirror and a color digital camera system. This system uses 8 bits in each of three colors, and is commercially available. (The D/N WSI uses 16 bits in each of four selectable wave bands.) In the late 1990s, the AOG developed a second generation daylight sky imager, called the daylight Visible/NIR WSI (VN WSI), for support of the UV applications mentioned above [5]. We will designate this day VN WSI to distinguish it from the day WSIs the AOG fielded throughout the 1980s. Day-only sky imagers have been developed by other groups for a variety of applications [25], including solar energy applications [26], mostly within the last decade. Many of these systems use algorithms based on the red/blue ratio [23,24,27] that was first implemented in the original AOG day WSI cloud algorithm in the 1980s [1]. For night use, at least one other group developed a visible system that can be used under starlight conditions [28]. Others have been working to develop D/N systems working in the thermal infrared (IR) [29,30]. However, we are not aware of any instruments other than the D/N WSI discussed here that can yet acquire both day and night cloud images in the visible and/or near infrared (NIR) wave bands, nor in our opinion provide cloud assessment with such accuracy at such a broad variety of locations.

Although this work has been published in many reports, it has not been readily accessible in the open literature. This paper will provide an overview of the development of the AOG WSI systems, provide detailed references, and give a brief discussion of other related capabilities. Emphasis is given to the description of the D/N WSI hardware systems. The radiometric calibrations, day cloud algorithms, night cloud algorithms, and other data products such as CFLOS computations will be briefly described here, and will be discussed in more detail in future articles.

2. Development of the WSI Concept and Related Systems

This section provides an overview of the development of systems that led to the D/N WSI, as well as an overview of the history of the cloud algorithms. The AOG used all-sky cameras using film and a silvered mirror in the 1960s in support of its atmospheric optics research. A film-based all-sky camera in use by the AOG in a 1963 deployment is shown in Fig. 1(a). Beginning about 1970, downward- and upward-looking sky imagers using a fisheye lens and film were used in support of the AOG's airborne programs. McGuffie and Henderson-Sellers [31] provide an overview of film-based whole sky imagers developed by other groups and used in the late 1980s.

A. Day WSI Development

The first digital WSI systems developed by the AOG were developed and deployed in the early 1980s. The original concept for the development of the day WSI in the AOG evolved out of the group's measurement and modeling program using multiple sensors for monitoring sky radiance distribution, atmospheric scattering coefficient profiles, and other parameters related to vision through the atmosphere [32–34]. (At that time, AOG was part of SIO's Visibility Laboratory, and it later became part of SIO's Marine Physical Laboratory, upon the closure of the Visibility Lab.) The first automated day WSIs were conceived by AOG as combining the features of the all-sky cameras [Fig. 1(a)] with the scanning radiometer systems that provided measurements of sky absolute radiance distribution.

The first day WSI systems developed by AOG used charge injection device (CID) solid-state imagers and a fisheye lens [11]. A system was fielded at White Sands Missile Range in 1984 for a 24-day deployment [2]. This system acquired digital images at blue (450 nm) and red (650 nm) wavelengths, as well as blue and red images offset with a neutral density (ND) filter to extend the effective dynamic range. This system was semiautomated. Cloud algorithms based on the red/blue ratio at each pixel were developed based on these 1984 data [2,11]. To the best of our knowledge, this system was the first digital WSI that was developed.

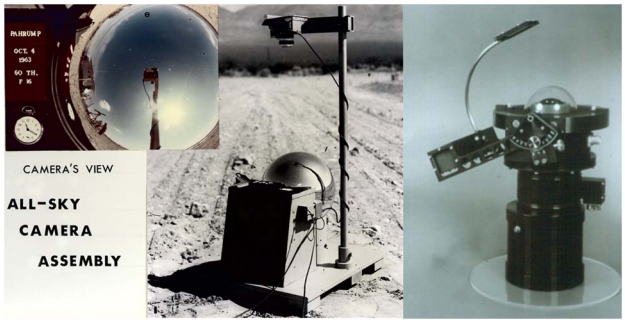

Fig. 1. (Color online) Two early WSI systems developed at MPL, the all-sky camera used in 1963, and the digital day WSI used in the 1980s.

The day WSI system was hardened as shown in Fig. 1(b) and fully automated, and fielded at seven sites starting in 1988 [2,3,12]. It used a fisheye lens, an optical filter changer, relay optics to provide the proper image size and image-plane location, and an equatorial sun occultor to provide shading for the fisheye lens. The sealed camera housing shown in Fig. 1(b) enabled the optics to be nitrogen purged and protected. Images of the sky were acquired at several sites at 1 min intervals for over 2 years. A sample raw image and the resulting cloud decision image are shown in Fig. 2. In these images, the zenith sky is the center of the image, and the edge of the horizon is just above the edge of the image. The image in Fig. 2 was acquired at Columbia, Missouri. Other day WSI's were sited at locations in Florida, Montana, and four sites in the Southwestern U.S.

Early versions of personal computers, in conjunction with an electronics package designated the Accessory Control Panel, enabled either manual or automated control of the lens iris, filter changer, and solar occultor. The automated control algorithm determined the optimal exposure, iris settings, and appropriate solar occultor settings; and provided hardware control, and image acquisition and archival. The data were saved to tape drives, and the archived data were processed through quality control (QC) programs, and then processed to yield cloud decision images [12,35–37], in which each pixel is identified as opaque cloud, thin cloud, no cloud, or no data. The instrument capabilities were first published in 1987 [1,11], and later references [2,3,12] are more complete.

B. Day WSI Cloud Algorithms and Database

The cloud algorithm initially developed in 1984 and improved over the subsequent years was based on ratios of red and blue images. Imaging algorithm studies at AOG revealed that although radiance and edge information were useful, the spectral information characterized by the red/blue ratio was most useful in development of the cloud algorithm for opaque clouds. During the following years of development in the 1980s, techniques for radiometric calibration of these imaging systems were developed. Nonlinearities in the CID camera response were measured and corrections applied as part of the cloud decision algorithm. Methods for determining the angular calibration for each pixel were developed, and the occultor was masked in the cloud decision image. The algorithm used a fixed red/blue ratio to identify opaque clouds. The thin cloud algorithm used a more sophisticated approach based on a comparison with cloudless days, and taking into account variations in haze [35]. These developments are discussed in more detail in the section on the development of the D/N WSI algorithms, since many of the features are used for both instruments. The daytime algorithms for opaque clouds based on the red/blue ratio were developed by 1986 [1,2,11,12]. The thin cloud algorithm was used in the late 1980s and first discussed in publications in 1990 [3,35,36].

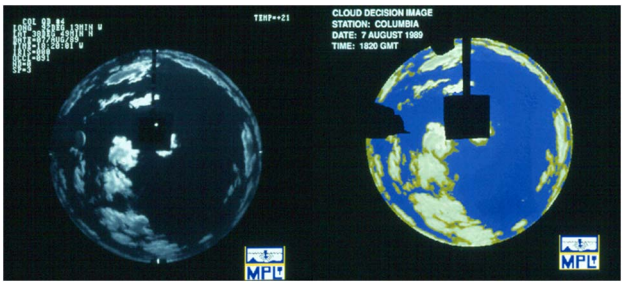

Fig. 2. (Color online) Sample raw and cloud decision images from the day WSI acquired in 1989 at Columbia, Missouri. The cloud decision image is the result of the cloud algorithm assessment of cloud at each pixel. Blue = no cld., Yellow = thin cld., Gray/white = opaque cld, Black = no data. (In B/W, no cld is gray, cld is white.)

The day WSI was used for a number of years in support of field tests, and to acquire a database of cloud data [37] that has been used to evaluate CFLOS statistics [21,38]. Out of this database, 96,000 images have been fully processed to yield cloud decision images at full spatial resolution, and approximately 10 times this number have been processed at reduced spatial resolution. This processed database consists of 2 years of data from each of four sites. The resulting CFLOS statistical analysis has since then been supplemented with D/N WSI data [21,22,39].

C. Day/Night WSI Development

Following the development of the day WSI, development was begun by the AOG on a D/N WSI system in 1991, in order to achieve full 24-h coverage. The first D/N WSI was deployed in 1992 [8–10]. During the period since the early 1990s the D/N WSI instruments continued to evolve in capability [4,17,21,38,40,41], and sophisticated cloud algorithms for daytime, moonlight, and starlight were developed and used to process a significant dataset [6,7,42–46]. The D/N WSI will be discussed in the remaining sections of this paper. The day VN WSI is not discussed further in this article, but is discussed in other references [5,18–20].

3. Day/Night WSI System Design and Operation

The D/N WSI was funded jointly by several sponsors with somewhat diverse applications. As a result it was designed to be very flexible in supporting several field applications. The most important hardware design goal was to acquire quality imagery of the sky under all conditions, day and night. From this imagery, the analysis design goal was to provide automated algorithms for detection of clouds in the scene, and absolute radiance distributions over the full sky if desired. All of these goals were met, except that the sunrise/sunset cloud algorithm looked feasible but was not developed due to other priorities.

One of the D/N WSI systems is shown in Fig. 3. The large semicircle is the solar/lunar occultor, which will be discussed later. The white box is the environmental housing. The optical dome may be

Fig. 3. (Color online) D/N WSI developed at MPL starting in the early 1990s.

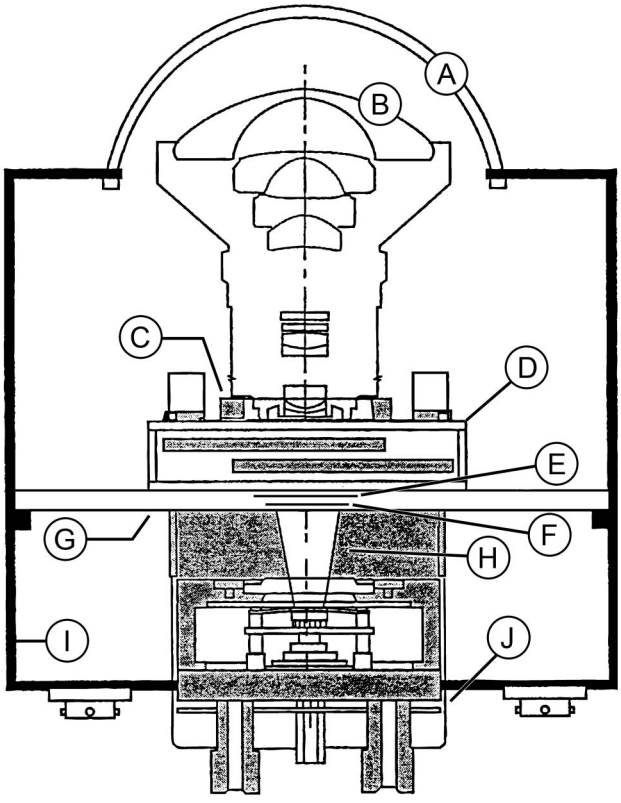

Fig. 4. D/N WSI camera housing. A, dome; B, fisheye lens; C, lens mounting plate; D, custom filter changer; E, shutter; F, IR blocking filter; G, image plane; H, fiber optic taper; I, camera housing body; J, camera.

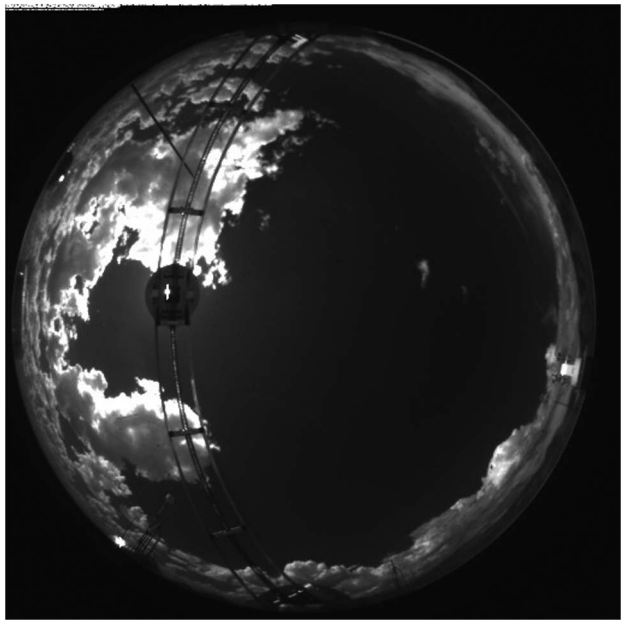

Fig. 5. Daytime image from the D/N WSI, 26 Jul 05 2200z.

seen in the middle of the top plate. The D/N WSI camera housing schematic is shown in Fig. 4. Sample images are shown in Figs. 5–8. Figures 5 and 6 show daytime data and moonlight data. Figure 7 shows starlight (no moon) data taken at a typical site a few miles from a city, and Fig. 8 shows starlight data from a very dark site. These figures are 8 bit renditions of the 16 bit image. Areas that may appear off-scale bright or dark in these 8 bit renditions are actually well on-scale in the original 16 bit digital image. Normally, the D/N WSI data were well on-scale under the brightest conditions (daylight with clouds near the sun) as well as the darkest conditions, with a signal/noise of about 40:1 in the dark

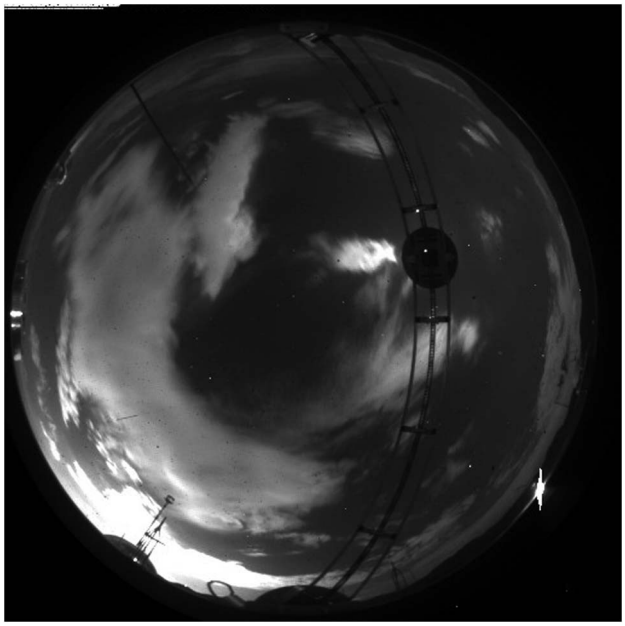

Fig. 6. Moonlight image from the D/N WSI, 27 Jul 05 1001z.

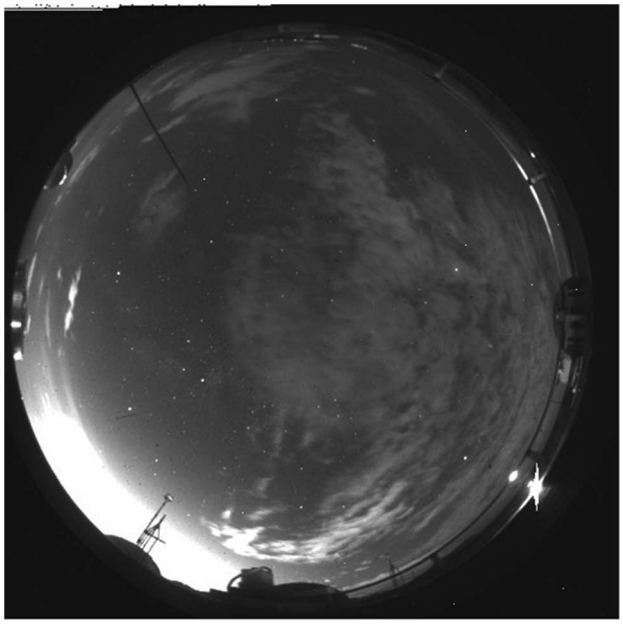

Fig. 7. Starlight image from the D/N WSI at a typical site, 14 Aug 05 0902z.

part of the sky between stars on a moonless night at our darkest sites.

The D/N WSI is fully automated, and acquires data continuously 24 h a day. It has been environmentally hardened and been used in the desert, the Arctic, tropics, and other environments. The lens covers the full upper hemisphere, down to just below the horizon (with a field of view of approximately 181.5 deg).

A. D/N WSI Hardware Description

Perhaps the most important component in the D/N WSI is the sensor. We initially experimented with a variety of image intensifiers; however, we found that the images were too noisy and unstable for our purposes. Instead, the system was designed around a Photometrics slow-scan 16 bit charge coupled device (CCD) camera. Early generations of the D/N WSI used the Series 200 Photometrics camera, and later ones used the Series 300. These cameras have over 65,000 gray levels, and a readout noise of less than one count, for a dynamic range of approximately 4.8 logs ($10^{4.8}$) within a single image. This camera has a three-stage Peltier cooler on the chip, and is cooled to approximately −40°C, so that it has very low thermally generated dark noise. There is no automatic gain or automatic white balance, because it would be very difficult to calibrate the camera if it had these features.

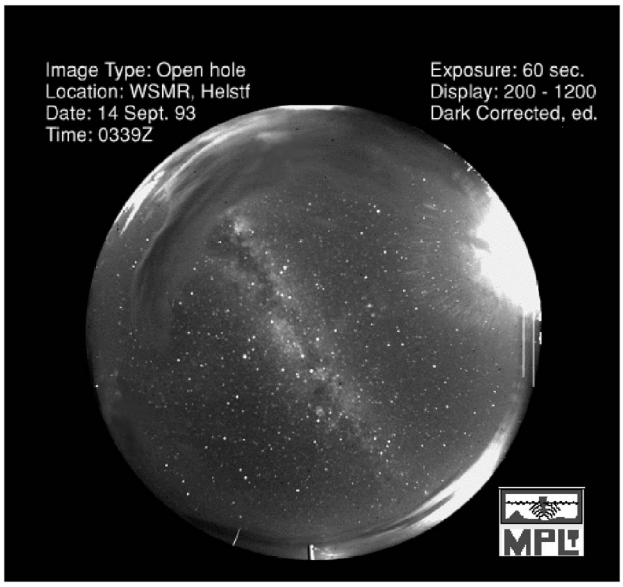

Fig. 8. Starlight image from the D/N WSI at a very dark site, 14 Sep 93 0339z. Blooming on upper right is from a city approximately 60 miles distant.

The exposure can be varied over a wide range. We typically used exposures of 100 ms for daytime images, and 60 s for night images in the open hole filter (discussed below). The shutter timing was found to be consistent to within 1 ms or better. By using a minimum exposure of 100 ms, we ensured that we were not introducing error due to the shutter timing uncertainties. By using a maximum exposure of 60 s, we minimized the impact of cloud motion. The change from 100 ms to 60 s exposures gave us an additional factor of 600 or 2.8 logs of dynamic range. Also, in calibration measurements, we found that the response was very consistent on repeat measurements and linear with both radiance and exposure changes, although we did have to make a correction to exposure to correct for the shutter opening time. The system used a Uniblitz VS25 mechanical shutter. A mechanical shutter avoids problems inherent to many cameras with electronic shutters, such as electronic readout smear. The mechanical shutter also enabled the acquisition of frequent dark images in the field for correction of the raw imagery.

The front optics consisted of a Nikon Fisheye-Nikkor 8 mm $f/2.8$ lens. It was chosen for its large throughput, to support night data acquisition, and its full hemispherical view. It was protected by an acrylic or glass dome. The custom glass domes used on some of the systems were considerably more costly, but the off-the-shelf acrylic domes used on other systems were more subject to scratching due to improper cleaning. Behind the lens was a dual-wheel filter changer designed and built by the AOG. This filter changer has one wheel with spectral filters, and a second wheel with ND filters. The spectral filters are normally blue (450 nm), red (650 nm), NIR (800 nm), and open hole (glass blank) for use at night. The ND wheel contains a selection of ND filters that reduce the flux levels by 0, approximately 2, or approximately 3 logs. Blank trim filters were included as necessary so that all selections had virtually the same physical thickness and thus the same image plane location. We gained an additional 3-log dynamic range by changing ND filters, and we gained an additional 0.6-log dynamic range by changing from the spectral filters in daytime and moonlight to open hole under moonlight and starlight.

Thus, with the approximately 3.6 logs from the filter changer selection, 2.8 logs from the exposure selection, and the 4.8-log dynamic range of the camera sensor, this yields approximately 11.2-log dynamic range of the system. (This can vary slightly from one system to another, so we normally reported a dynamic range of over 10 logs.) That is, within a single image the dynamic range was 4.8 log, but within the full system as built, the dynamic range was well over 10 logs. The dynamic range could be further extended with either shorter or longer exposures outside the 100 ms to 60 s range, but we did not find this to be necessary. Daytime clouds near the sun were rarely if ever off-scale bright. As noted earlier, at night under starlight, the darkest part of the sky between clouds typically had an SNR of about 40:1 at the darkest sites (taking into account readout, dark, and shot noise).

One of the critical issues in WSI design was getting the full image onto the chip. Current versions of the D/N WSI use a fiber-optic taper bonded to the chip. This bonding was done by Photometrics, using interferometry to match the shape of the bonded end of the fiber-optic taper to the nearly flat shape of the CCD chip. The taper was used because the CCD chips available at the time had much smaller dimensions than the lens output images. Also, we wanted to use the full back focal length of the lens for filters. The bonded taper both magnifies the image plane for compatibility with the Nikon lens image, and brings the image plane up out of the camera to allow room for both filter wheels and the shutter. Larger chips, as well as custom fisheye lenses, offer alternate approaches at the present time, and we have substituted relay optics effectively in the day VN WSI system. With both the current D/N WSI and the day VN WSI, we developed techniques for measuring the defocus, or point spread function, and found it to be approximately 0.5 pixel or better (i.e., less) over all regions of the image.

Like the old day WSI, the D/N WSI uses a sealed and nitrogen-purged camera housing. The housing is a 10″ diameter o-ring-sealed housing that holds the lens, filters, and upper half of the camera. A custom o-ring in the camera body permits the housing to be sealed, while allowing the back end of the camera to extend beyond the housing for easy access to the cooling ports. This generation of the camera requires liquid cooling, as well as a camera electronics unit near the camera body. An environmental housing protects and cools these additional elements. The environmental housing is the large white box seen in Fig. 3. With this environmental housing, WSI units have operated for extended periods in harsh environments, such as the desert and the Arctic. There are transducers inside the housing that monitor the environmental housing temperature, camera housing temperature, CCD chip temperature, coolant flow rate, and camera housing pressure. If any of these indicators fall below optimal thresholds, the user is alerted and the information is saved to QC files and image headers. If critical indicators fall below safe levels, the camera is automatically turned off by the computer to protect it, and then turned back on when the indicators recover. This happened rarely, but was an important safety feature.

The solar/lunar occultor provides full shading of the front optics including the dome, in order to minimize stray light. A much smaller shade could protect the CCD from blooming due to direct sunlight. Shading the full extent of the front optics minimizes stray light contamination in the remainder of the image. [This is one reason the WSI does not use a silvered mirror instead of a lens. As can be visualized from Fig. 1(a), it is typically not feasible to shade the full mirror, so only secondary optics, i.e., the camera lens and internal surfaces, are shaded in systems using hemispherical mirrors.] The D/N WSI sun shade is fitted with a 4-log ND filter to enable detecting the actual solar position. We used the Nikon lens in order to have a large front aperture, but the price we pay for this is that the lens shade must be large. Thus, the shade must be held at a reasonably large distance from the lens so that it does not obscure excessive fractions of the sky dome.

It is as important to shade the moon as it is to shade the sun, since its brightness relative to the sky radiance is often equivalent to the brightness of the sun relative to the daytime sky radiance. The day WSI's occultor depended on a single equatorial drive to adjust to time of day, and it required different length arms that needed changing every 3 weeks to 3 months to adjust for changing solar declination. With a D/N system, it is necessary to adjust from the solar declination to the lunar declination every sunrise and sunset. Thus it was necessary to build an occultor that includes two drives, or degrees of freedom. This is achieved with an arc that moves from east to west, and a chain-driven "trolley" that holds the sun shade and moves from north to south. In particularly difficult environments such as the Arctic, a larger fixed shade replaced the trolley. The size of the shade was site-specific, and designed to cover the maximum motion of the sun and moon for that site. Although having an occultor adds to the cost and obscures a small fraction of the sky, for our applications it was important, as it provided more accurate results over most of the sky, especially in the solar aureole regions just beyond the occultor shade.

The D/N WSI hardware design provided many advantages. In comparison with many daytime systems, stray light was minimized both over the whole sky and near the sun, and data were not off-scale bright near the sun. As a result, we were able to develop algorithms that work well even in the difficult region near the sun. Because the camera had such low noise, and the system had excellent throughput, we acquired excellent imagery at night and were able to develop high-quality nighttime cloud algorithms. The ability to include a variety of filters including an NIR filter enabled us to provide better detection of thin clouds and to distinguish between thin clouds

and haze both day and night. In comparison with IR systems, we were not plagued by water vapor signatures that can be very difficult to distinguish from thin clouds in haze. The trade-off was that it is not inexpensive to build systems with these qualities. Clearly decisions regarding the importance of the cost-quality trade-off will depend on the applications and the needs of sponsors.

B. D/N WSI Control System

The WSI control software controls the filter changer, occultor, camera, and exposures. A global positioning system (GPS) was integrated into the system to determine time and location. This information was fed into the occultor logic, as well as a flux control algorithm (discussed below). The control software also monitored the environmental housing transducers, and provided a number of other system assessments designed to automatically QC the state of the instrument and imagery. On the fully mature systems, the monitor display showed green, yellow, or red indicators to indicate system status and provide convenient on-site feedback. Image headers were used to save a record of all instrument settings as well as QC results within each image.

The flux control algorithm was designed to select appropriate exposures and filters in order to keep the acquired images well on-scale. With earlier day WSI systems, we found we had to use a "responsive" flux control logic, in which a nominal exposure and gain or f/stop setting (depending on the hardware) was tested, and then modified as necessary depending on the current weather conditions. We found that the D/N WSI with its 16 bit sensor had sufficient dynamic range to acquire quality images under all weather conditions, as long the system was adjusted for the time of day. Thus, a "predictive" flux control algorithm was developed based on the calculated solar and lunar zenith angles, moon phase, and moon relative brightness. The algorithm was based in part on previous measurements of total illuminance for sunlight, full moon, and starlight [47]; studies of diffuse versus total illuminance [48]; and studies of moon relative brightness [49]; along with analysis of D/N WSI field data. D/N WSI calibration measurements were analyzed to determine the necessary system setup changes to respond to the predicted changing flux levels.

In the field, the GPS provided the time and location, and the algorithm computed the solar and lunar positions, and the lunar relative flux based on moon phase and earth-to-moon distance. Using this information, the flux control algorithm chose the appropriate selection of exposure and filters. During daytime, exposures of 100 ms with a 3-log ND filter were used. As the solar zenith angle increased toward sunset, the exposures were increased, until the system switched to short exposures and a 2-log ND filter. Additional exposure, ND filter, and spectral filter changes responded to the changing source parameters. Under starlight, the system used no ND filter, exposures of 60 s, and an open-hole configuration with no spectral filter. The added use of a 4-log ND filter in the occultor to attenuate the direct view to the solar or lunar disk nearly always resulted in the data being on-scale over the full range of conditions.

C. D/N WSI Deployments

Over the years, the D/N WSI systems were deployed at approximately 15 sites, for a number of sponsors mentioned earlier. For some sponsors, we were not permitted to install the instruments at the sites or do routine inspections, and this resulted in less reliability than we were comfortable with. However, for sponsors who permitted our group to install the instruments and do yearly inspections, the instruments were quite reliable. Typically, routine inspection was performed every few weeks by on-site personnel, and minor repairs or adjustments were required once or twice a year, depending in part on problems like lightning strikes. The weakest components were the occultor trolley, which required occasional adjustment, and the shutter, which required occasional replacement (with replacement needed every 2–5 years). Also, on systems with an acrylic dome, replacement was required every 1–5 years.

4. Overview of D/N WSI Data Products and Algorithms

A number of data products have been developed for the WSI. The most important of these are the cloud algorithm results. In the present article, we will provide a very brief overview of the algorithms and data products. We plan to publish more detailed descriptions of the calibrations, day and night algorithms, and derived CFLOS statistics in the future. We will only discuss the algorithms that our group developed, as opposed to algorithms that other groups might have developed for these instruments. We will be discussing the final generation of algorithms [7].

A. Daytime Cloud Algorithms

Initial cloud algorithms used a fixed threshold for red/blue calibrated ratio [35]. This worked best for optically opaque clouds. By the late 1980s, AOG was developing an algorithm to better account for variations in thin cloud spectral signature [36]. The thin clouds were found to behave as a perturbation with respect to the clear sky background ratio. That is, the red/blue ratio for a clear sky varies with look angle and solar position, tending toward higher ratios near the solar aureole and near the horizon. We found that thin clouds that appear uniform, such as contrails that extended over wide angles, were characterized by a red/blue ratio about 20% higher than the background clear sky ratio. A technique was developed for extracting a clear sky background ratio that depends primarily on instrument site, solar zenith angle, look angle, and haze amount. In the day WSI, the background ratio was then adjusted on a day-to-day basis to adjust for relative

haze amount. The field image ratio was then divided by the appropriate haze-adjusted background ratio, to create a "perturbation" ratio, which represents the fractional change of the current sky red/blue ratio with respect to the clear sky red/blue ratio. This perturbation ratio was thresholded to determine the presence of thin clouds. A sample day WSI cloud algorithm result is shown in Fig. 2.

The D/N WSI algorithm for identifying clouds in the daytime is based primarily on the day algorithm, but it has significant improvements. The algorithm makes calibration corrections, to correct for hardware artifacts. Opaque cloud detection is now based on a NIR/blue ratio threshold. Thin cloud detection is based on a perturbation ratio which is a comparison between the NIR/blue ratio image and a composite clear sky NIR/blue ratio image. The composite clear sky ratios, extracted for each site, were stored as a function of solar angle and look angle. The daytime cloud algorithm for the D/N WSI also includes an automated adaptive algorithm feature that invokes spatial variance to determine an image-by-image adaptive adjustment for haze amount [6,7]. That is, the algorithm automatically adjusts for variations in the aerosol or haze.

Two daytime cloud algorithm results with their raw images are shown in Figs. 9 and 10. In these images, pixels identified as opaque cloud, thin cloud, no cloud, and no data, are colored gray-to-white, yellow, blue, and black, respectively. The structure within each category in the cloud algorithm image is only intended to be an aid in evaluating the results. For example, within the opaque cloud, the colors vary from gray to white in the display. Note in particular the ability of the algorithm to detect thin clouds quite well. Generally, there is very little bias as a function of scattering angle from the sun with this algorithm. Also, note the ability to extract very small clouds, all the way to the horizon.

B. Night Cloud Algorithms and Beam Transmittance

The D/N WSI algorithm for identifying clouds at night is based on the detection of stars and the absolute radiance distribution over the sky. The earth-to-space beam transmittance is determined for approximately 100–200 stars. Star locations are determined with the aid of a very accurate angular calibration and the use of a bright star catalog [50]. The catalog is further used to provide anticipated star magnitude and color temperature, which are required for the determination of the beam transmittance. These transmittances are used to assess whether there are no clouds, thin clouds, or opaque clouds in the direction of each star.

This initial step provides an assessment in the direction of the selected stars. To provide full resolution assessment, we use the measured absolute radiance. The sky absolute radiance distribution is mapped for regions in the image with either opaque cloud or no cloud, for both moonlight and starlight. The moonlight maps are a function of moon phase and relative brightness, and the starlight maps are a function of hour angle. Both vary with source position and look angle. These radiance maps are then used to determine the presence of clouds on a pixel-by-pixel basis. A pixel is interpreted to be covered by thin cloud when the absolute radiance lies between that of opaque cloud and that of clear sky. An adaptive algorithm feature also adjusts for haze amount on an image-by-image basis. The nighttime cloud algorithm also accounts for increased radiances in the Milky Way. Both the beam transmittance distribution and the cloud algorithm result were provided as processed data products [6,7]. As mentioned earlier, the algorithms will be discussed in more detail in future articles.

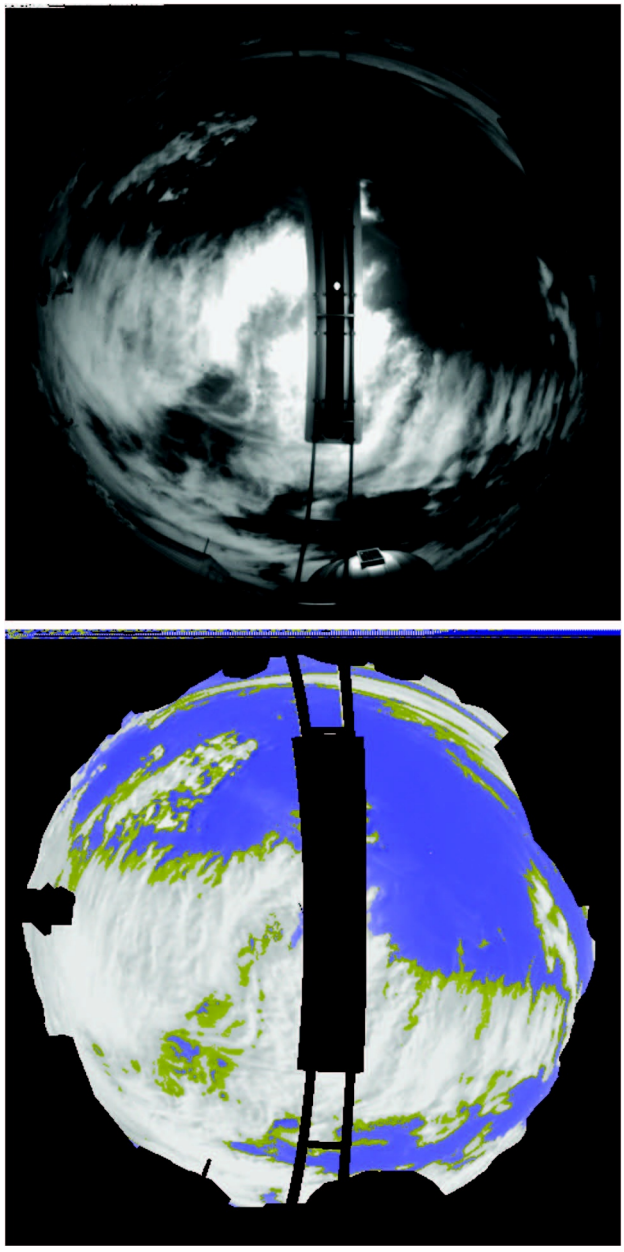

Fig. 9. Daytime image pair illustrating a raw image and the associated cloud algorithm result, 19 May 06 1700z.

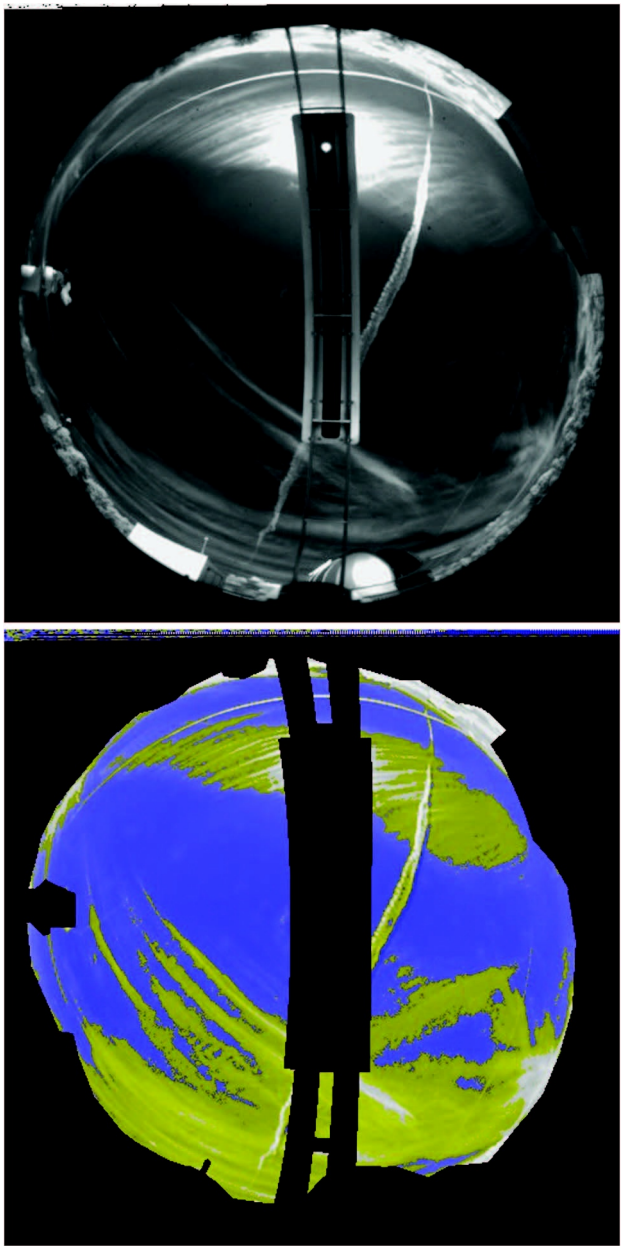

Fig. 10. Daytime image pair illustrating a raw image and the associated cloud algorithm result with contrails developing into thin clouds, 19 Nov 2007 1700z.

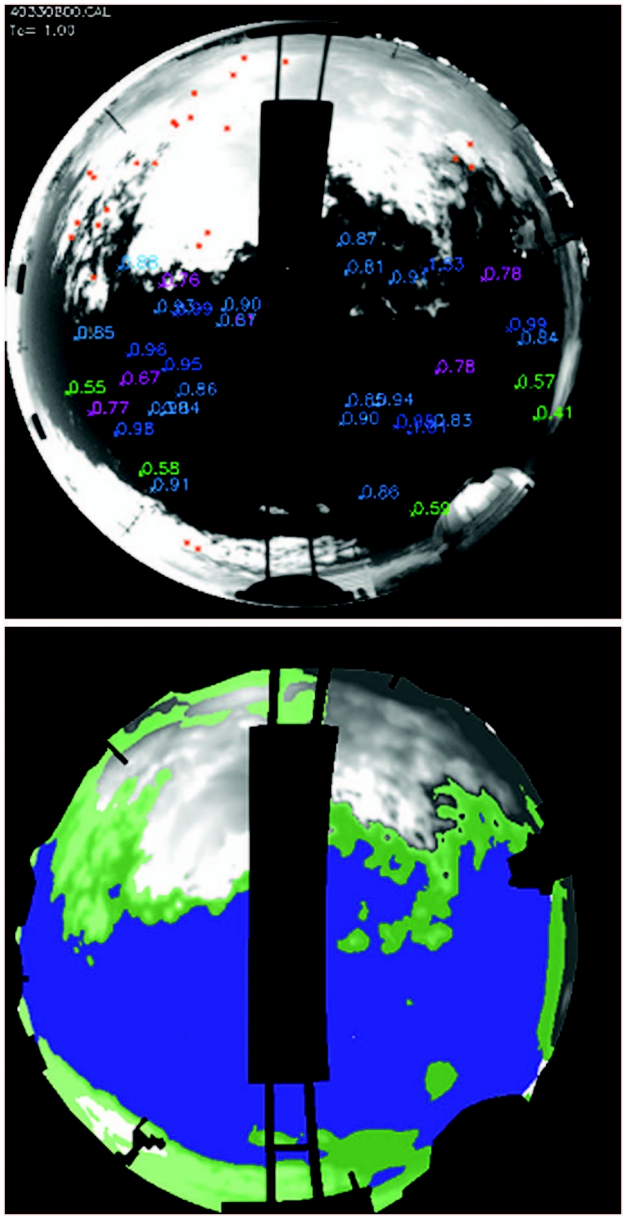

Fig. 11. Moonlight image pair illustrating a raw image with transmittance map and the associated cloud algorithm result, 2 Feb 2008 0800z.

An example of the cloud algorithm result under moonlight is shown in Fig. 11. In the upper image, the earth-to-space beam transmittance distribution is superimposed on the raw image. In the lower image, the cloud algorithm result is shown. Here gray-to-white indicates a determination of opaque cloud, green indicates thin cloud, blue indicates no cloud, and black indicates no data. As is typical with automated cloud detection schemes, the nighttime cloud algorithm is not perfect, but it generally does a very nice job under all conditions. It does require a fair amount of data analysis in order to set up the data for processing, but once the inputs are set up the data can be processed automatically.

5. Comparison with Related Cloud Detection Approaches

This article is not intended to provide a general overview of the pros and cons of the various sky imagers that have been developed. However, some brief comments are in order. The D/N WSI is the only visible sky imaging system we are aware of that acquires quality data under daylight, moonlight, and starlight conditions. In comparison with the TSI and other day-only systems we are aware of, the D/N WSI has much larger dynamic range, and much better stray light blocking, with the result that better data near the sun are acquired. The D/N WSI uses an NIR filter, in order to optimize thin cloud detection. And the algorithms are generally

quite sophisticated due to the years of work in the field.

In comparison with the visible night systems, the D/N WSI has the advantage of providing both day and night detection, including moonlight as well as starlight. The thermal IR systems seem promising, but analysis [46] showed that automated cloud algorithms would be problematic in the IR, in part due to the difficulty in distinguishing very thin clouds from water vapor in the IR, particularly at low-altitude and coastal sites. Also, IR systems seem unlikely to provide earth-to-space beam transmittance. The D/N WSI provides beam transmittance and optical density for clear or hazy sky and through thin clouds at night. Concepts for providing optical density in the daytime were also developed by AOG and look practical, but the methods were not completed due to other priorities. On the other hand, the D/N WSI is more costly to produce than other systems.

Cloud lidars and cloud radars can be extremely useful in cloud studies, but cannot achieve the simultaneous 100,000 measurements over the full sky that the WSI can. Satellites obviously provide tremendous information regarding cloud cover, but limited temporal and spatial resolution makes their use unsatisfactory for some applications. Also, if a given directional line of sight from a ground-based site is required, this information often cannot readily be obtained from satellite data due to the acquisition angles. Additionally, due to the different geometry, satellites do not provide cloud distribution within the field of view of a ground-based radiation sensor.

Clearly the system to use in cloud studies depends on the application, technical requirements, and cost considerations. We believe the D/N WSI is unique in providing high-quality data "24/7", with excellent raw data as well as accurate cloud algorithms results for day and night. Its ability to acquire data over the whole sky down to the horizon under all conditions makes it a valuable instrument for a variety of applications. The systems are not currently available, but we hope to provide sufficient details in future articles that the concepts can be used by other researches for applications in the future.

6. Related Developments at MPL

Several related hardware developments at MPL were based in part on the day WSI and the follow-on D/N WSI work. These included a system that provided real-time cloud algorithm results in the late 1980s [35], and systems for determining visibility along extended paths through the atmosphere in the early 1990s [51,52]. In the late 1990s, a new daytime VN WSI was developed at MPL to replace the day-only WSI with more modern capabilities [5,18–20]. This system was developed for the German Weather Service, Deutsche Wetterdienst, in support of cloud and sky radiance studies. It acquires data at higher bit density and spatial resolution and in more spectral bands than the previous day WSI, and uses more modern CCD and computer technology.

In the early 2000s, visible and short-wave IR airborne sensors were developed by the AOG to provide calibrated radiances in the lower hemisphere in the visible at 645 nm and in the short-wave IR at 1610 nm [53]. These systems used fisheye lenses and a single spectral filter in each sensor system. Also in the early 2000s, the AOG began development on improved visibility systems [54]. More recently, two updated visibility imaging sensors, the multispectral scattering imager and the short-wave IR extinction imager have been developed at MPL using similar concepts to the earlier visibility system, but with updated hardware and more sophisticated algorithms [55]. Also, in the early 2000s, the AOG developed and patented the concepts for a zooming fisheye sensor that would enable one to obtain a full hemispherical view while simultaneously using behind-the-lens optics to provide optically zoomed images of selected regions of the image [56].

We would also like to mention related analytical work by others in conjunction with the AOG group. Early work in the use of stereoscopy techniques with paired WSI systems [57] was limited due to slow computer speed; however, more recent approaches [58] show promise. Also, D/N WSI data calibrated for absolute radiance were used to develop methods for extracting aerosol optical depth in the daytime [59]. Fairly extensive analysis of the algorithms, CFLOS results, and other related data analysis are included in many of the WSI references listed earlier.

7. Summary

This article provides an overview of the development of digital and automated WSIs at the MPL with a particular emphasis on the D/N WSI. The original day WSI systems were developed in the early 1980s, and we believe they were the first multispectral digital WSIs developed. The red/blue cloud algorithm technique was also developed in 1984, and has been used by many other groups since that time. The D/N WSI systems were developed in the early 1990s, and are still unique in their capability of measuring clouds in the visible 24 h a day. Sophisticated and reasonably accurate algorithms for both day and night were developed, and include adaptive algorithm features to correct for haze amount. These cloud algorithms detect opaque and thin clouds day and night. Methods to determine beam transmittance were also developed for nighttime imagery. Preliminary analysis showed that methods for determining beam transmittance in the daytime and for developing cloud algorithms for sunrise/sunset are feasible. These very capable instruments and their sophisticated algorithms have been used for many programs, in support of a variety of test sites and research objectives.

The authors would like to thank our many sponsors, including the Air Force Phillips Laboratory, the Air Force Geophysics Laboratory, the Air Force Research Laboratory and the Starfire Optical Range, the Office of Naval Research, the Deutsche Wetterdienst, the

Department of Energy's Atmospheric Radiation Program, and Boeing SVC. Also, the authors would like to thank the many talented and dedicated individuals working within the AOG who have contributed to these systems over the years: Justin Baker, Melissa Ciandro, John Fox, Wayne Hering, Thomas Koehler, Brad Kroeger, Vincent Mikuls, David Sauer, Daniel Schickele, Harry Sprink, Jake Streeter, Jack Varah, Jason Wertz, Richard Weymouth, and Eugene Zawadzki. The authors also thank the administrative staff of MPL, without whose support this work could not have been done.

References

1. R. W. Johnson and W. S. Hering, "Automated cloud cover measurements with a solid-state imaging system," in *Sixth Symposium Meteorological Observations and Instrumentation* (American Meteorological Society, 1987), pp. 96–99.
2. R. W. Johnson, W. S. Hering, and J. E. Shields, "Automated visibility and cloud cover measurements with a solid state imaging system," University of California, San Diego, Scripps Institution of Oceanography, Marine Physical Laboratory, SIO 89-7, GL-TR-89-0061, NTIS No. ADA216906 (1989).
3. J. E. Shields, R. W. Johnson, and T. L. Koehler, "Automated whole sky imaging systems for cloud field assessment," in *Fourth Symposium on Global Change Studies* (American Meteorological Society, 1993), pp. 228–231.
4. J. E. Shields, R. W. Johnson, M. E. Karr, and J. L. Wertz, "Automated day/night whole sky imagers for field assessment of cloud cover distributions and radiance distributions," in *Tenth Symposium on Meteorological Observations and Instrumentation* (American Meteorological Society, 1998), pp. 165–170.
5. J. E. Shields, R. W. Johnson, M. E. Karr, A. R. Burden, and J. G. Baker, "Daylight visible/NIR whole sky imagers for cloud and radiance monitoring in support of UV research programs," Proc. SPIE **5156**, pp. 155–166 (2003).
6. J. E. Shields, M. E. Karr, A. R. Burden, R. W. Johnson, V. W. Mikuls, J. R. Streeter, and W. S. Hodgkiss, "Research toward multi-site characterization of sky obscuration by clouds, final report for grant N00244-07-1-009," Marine Physical Laboratory, Scripps Institution of Oceanography, University of California, San Diego, DTIS (Stinet) File ADA126296 (2009).
7. J. E. Shields, M. E. Karr, A. R. Burden, V. W. Mikuls, J. R. Streeter, R. W. Johnson, and W. S. Hodgkiss, "Scientific report on whole sky imager characterization of sky obscuration by clouds for the Starfire optical range, scientific report for AFRL contract FA9451-008-C-0226," Marine Physical Laboratory, Scripps Institution of Oceanography, University of California, San Diego, Technical Note 275, DTIS (Stinet) File ADA556222 (2010).
8. J. E. Shields, R. W. Johnson, and T. L. Koehler, "Imaging systems for automated 24-hour whole sky cloud assessment and visibility determination," in *Proceedings of the Cloud Impacts on DOD Operations and Systems—1991 Conference* (Phillips Laboratory, Directorate of Geophysics, Air Force Materiel Command, Hanscom Air Force Base, 1991), pp. 137–142.
9. K. M. Watson, "Upgrade of the LIMDAS day/night whole sky imager," Final Report to the Office of Naval Research Contract N00014-89-D-0142, Marine Physical Laboratory, Scripps Institution of Oceanography, University of California, San Diego, MPL-U-30/93, NTIS No. ADA265871 (1993).
10. J. E. Shields, R. W. Johnson, and M. E. Karr, "Automated whole sky imagers for continuous day and night cloud field assessment," *Proceedings of the Cloud Impacts on DOD Operations and Systems- 1993, Conference* (Phillips Laboratory, Directorate of Geophysics, Air Force Materiel Command, Hanscom Air Force Base, 1993), pp. 379–384.
11. R. W. Johnson and W. S. Hering, "Automated cloud cover measurements with a solid-state imaging system," *Proceedings of the Cloud Impacts on DOD Operations and Systems—1987, Workshop* (Atmospheric Sciences Division, Air Force Geophysics Laboratory, Air Force Systems Command, Hanscom Air Force Base, 1987), pp. 59–69.
12. R. W. Johnson, T. L. Koehler, and J. E. Shields, "A multistation set of whole sky imagers and a preliminary assessment of the emerging data base," in *Proceedings of the Cloud Impacts on DOD Operations and Systems, 1988 Workshop* (Science and Technology Corporation, 1988), pp. 159–162.
13. I. Lund, "Persistence and recurrence probabilities of cloud-free and cloudy lines-of-sight through the atmosphere," J. Appl. Meteorol. **12**, pp. 1222–1228 (1973).
14. J. W. Snow, "Modeling the variation of cloud cover with view angle using space shuttle cloud imagery," Geophysics Laboratory, Hanscom AFB, MA, GL-TR-90-0130, NTIS No. ADA227895 (1990).
15. J. E. Shields, R. W. Johnson, and M. E. Karr, "Upgrading the day/night whole sky imager from manual/interactive to full automatic control," Final Report to the Office of Naval Research Contract N00014-89-D-0142 (DO #18), Marine Physical Laboratory, Scripps Institution of Oceanography, University of California, San Diego, MPL-U-140/94, NTIS No. ADA292296 (1994).
16. J. E. Shields, R. W. Johnson, M. E. Karr, R. A. Weymouth, and D. S. Sauer, "Delivery and development of a day/night whole sky imager with enhanced angular alignment for full 24 hour cloud distribution assessment," Final Report to the Office of Naval Research Contract N00014-93-D-0141-DO#11, Marine Physical Laboratory, Scripps Institution of Oceanography, University of California, San Diego, MPL-U-8/97, NTIS No. ADA333269 (1997).
17. J. E. Shields, M. E. Karr, T. P. Tooman, D. H. Sowle, and S. T. Moore, "The whole sky imager—a year of progress," in *Proceedings of the Eighth Atmospheric Radiation Measurement (ARM) Science Team Meeting* (United States Department of Energy, Office of Energy Research, Office of Health and Environmental Research, Environmental Sciences Division, 1998), pp. 677–685.
18. U. Feister, J. E. Shields, M. E. Karr, R. W. Johnson, K. Dehne, and M. Woldt, "Ground-based cloud images and sky radiances in the visible and near infrared region from whole sky imager measurements," EUMP31, EUMETSAT Satellite Application Facility Workshop, Dresden, Germany, 20–22 November 2000 (2000), pp. 79–88.
19. U. Feister and J. Shields, "Cloud and radiance measurements with the VIS/NIR Daylight Whole Sky Imager at Lindenberg (Germany)," Meteor. Z **14**, 627–639 (2005).
20. U. H. Feister, H. Möller, T. Sattler, J. E. Shields, U. Görsdorf, and J. Güldner, "Comparison of macroscopic cloud data from ground-based measurements using VIS/NIR and IR instruments at Lindenberg, Germany," Atmos. Res. **96**, 395–407 (2010).
21. J. E. Shields, M. E. Karr, A. R. Burden, R. W. Johnson, and J. G. Baker, "Analysis and measurement of cloud free line of sight and related cloud statistical behavior, final report to the Office of Naval Research contract N00014-89-D-0142 (DO #2)," University of California, San Diego, Scripps Institution of Oceanography, Marine Physical Laboratory, ADA425400 (2003).
22. J. E. Shields, A. R. Burden, R. W. Johnson, M. E. Karr, and J. G. Baker, "Measurement and evaluation of cloud free line of sight with digital whole sky imagers," *The Battlespace Atmospheric and Cloud Impacts on Military Operations (BACIMO) Conference*, Monterey, California, 12–14 October 2005, http://www.nrlmry.navy.mil/bacimo.html (2005).
23. C. N. Long and J. J. DeLuisi, "Development of an automated hemispheric sky imager for cloud fraction retrievals," in *Tenth Symposium on Meteorological Observations and Instrumentation* (American Meteorological Society, 1998), pp. 171–174.
24. G. Pfister, R. L. McKenzie, J. B. Liley, W. Thomas, B. W. Forgan, and C. N. Long, "Cloud coverage based on all-sky imaging and its impact on surface solar irradiance," J. Appl. Meteorol. **42**, 1421–1434 (2003).
25. A. Cazorla, F. J. Olmo, and L. Alados-Arboledas, "Development of a sky imager for cloud cover assessment," J. Opt. Soc. Am. A **25**, 29–39 (2008).

26. J. Kleissl, *Solar Resource Assessment and Forecasting* (Elsevier, 2013).
27. C. W. Chow, B. Urquhart, M. Lave, A. Dominguez, J. Kleissl, J. E. Shields, and B. Washom, "Intra-hour forecasting with a total sky imager at the UC San Diego solar test bed," Sol. Energy **85**, 2881–2893 (2011).
28. R. Pérez-Ramírez, R. J. Nemiroff, and J. B. Rafert, "Nightskylive.net: the night sky live project," Astron. Nachr. **325**, 568–570 (2004).
29. K. S. J. Anderson, J. Brinkmann, M. Carr, D. Woods, D. P. Finkbeiner, J. E. Gunn, C. L. Loomis, D. Schlegel, and S. Snedden, "Apache Point observatory's all-sky camera: observing clouds in the thermal infrared," Bull. Am. Astron. Soc. **34**, 1130–1164 (2002).
30. P. W. Nugent, J. A. Shaw, and S. Piazzolla, "Infrared cloud imaging in support of Earth-space optical communication," Opt. Express **17**, 7862–7872 (2009).
31. K. McGuffie and A. Henderson-Sellers, "Almost a century of 'imaging' clouds over the whole-sky dome," Bull. Am. Meteorol. Soc. **70**, 1243–1253 (1989).
32. S. Q. Duntley, R. W. Johnson, and J. I. Gordon, "Airborne measurements of optical atmospheric properties in Southern Illinois," University of California, San Diego, Scripps Institution of Oceanography, Visibility Laboratory, SIO Ref. 73-24, AFCRL- TR-0422, NTIS No. AD-774-597 (1973).
33. S. Q. Duntley, R. W. Johnson, and J. I. Gordon, "Airborne measurements of optical atmospheric properties in Northern Germany," University of California, San Diego, Scripps Institution of Oceanography, Visibility Laboratory, SIO Ref. 76-17, AFGL- TR-0188, NTIS No. ADA-035-571 (1976).
34. R. W. Johnson, W. S. Hering, J. I. Gordon, B. W. Fitch, and J. E. Shields, "Preliminary analysis and modeling based upon project OPAQUE profile and surface data," University of California, San Diego, Scripps Institution of Oceanography, Visibility Laboratory, SIO Ref. 80-5, AFGL- TR-0285, NTIS No. ADB-052-1721 (1980).
35. J. E. Shields, T. L. Koehler, and R. W. Johnson, "Whole sky imager," in *Proceedings of the Cloud Impacts on DOD Operations and Systems, 1989/90 Conference* (Science and Technology Corporation, Meetings Division, 101 Research Drive, 1990), pp. 123–128.
36. T. L. Koehler, R. W. Johnson, and J. E. Shields, "Status of the whole sky imager database," in *Proceedings of the Cloud Impacts on DOD Operations and Systems, 1991 Conference* (Phillips Laboratory, Directorate of Geophysics, Air Force Materiel Command, Hanscom Air Force Base, 1991), pp. 77–80.
37. R. W. Johnson, J. E. Shields, and T. L. Koehler, "Analysis and interpretation of simultaneous multi-station whole sky imagery," University of California, San Diego, Scripps Institution of Oceanography, Marine Physical Laboratory, SIO 91-33, PL-91-2214, NTIS No. ADA253658 (1991).
38. J. E. Shields, R. W. Johnson, M. E. Karr, A. R. Burden, and J. G. Baker, "Whole sky imagers for real-time cloud assessment, cloud free line of sight determinations and potential tactical applications," *The Battlespace Atmospheric and Cloud Impacts on Military Operations (BACIMO) Conference*, Monterey, California, 12–14 October 2005, http://www.nrlmry.navy.mil/bacimo.html (2003).
39. J. E. Shields, A. R. Burden, R. W. Johnson, M. E. Karr, and J. G. Baker, "New cloud free line of sight statistics measured with digital whole sky imagers," Proc. SPIE **5891**, 58910M (2005).
40. J. E. Shields, R. W. Johnson, and M. E. Karr, "Service support for the Phillips laboratory whole sky imager," Marine Physical Laboratory, Scripps Institution of Oceanography, University of California, San Diego, MPL-U-10/97, NTIS No. ADA333283 (1997).
41. J. E. Shields, M. E. Karr, A. R. Burden, R. W. Johnson, and J. B. Baker, "Project report for providing two day/night whole sky imagers and related development work for Starfire optical range, final report to the Office of Naval Research contract N00014-97-D-0350 (DO #6)," University of California, San Diego, Scripps Institution of Oceanography, Marine Physical Laboratory, ADA not assigned (2004).
42. J. E. Shields, M. E. Karr, A. R. Burden, R. W. Johnson, and J. B. Baker, "Analytic support of the Phillips Lab whole sky imager 1997-2001, final report to the Office of Naval Research contract N00014-97-C-0385," University of California, San Diego, Scripps Institution of Oceanography, Marine Physical Laboratory, ADA425323 (2002).
43. J. E. Shields, A. R. Burden, M. E. Karr, R. W. Johnson, and J. B. Baker, "Development of techniques for determination of nighttime atmospheric transmittance and related analytic support for the whole sky imager, final report to the Office of Naval Research contract N00014-01-D-0043 (DO #5)," University of California, San Diego, Scripps Institution of Oceanography, Marine Physical Laboratory, ADA not assigned (2004).
44. J. E. Shields, M. E. Karr, A. R. Burden, R. W. Johnson, and W. S. Hodgkiss, "Enhancement of near-real-time cloud analysis and related analytic support for whole sky imagers, final report for ONR contract N00014-01-D-0043 DO #4," Marine Physical Laboratory, Scripps Institution of Oceanography, University of California, San Diego, ADA468076 (2007).
45. J. E. Shields, M. E. Karr, A. R. Burden, R. W. Johnson, and W. S. Hodgkiss, "Whole sky imaging of clouds in the visible and IR for Starfire optical range, final report for ONR contract N00014-01-D-0043 DO #11," Marine Physical Laboratory, Scripps Institution of Oceanography, University of California, San Diego, ADA470314 (2007).
46. J. E. Shields, M. E. Karr, A. R. Burden, R. W. Johnson, and W. S. Hodgkiss, "Continuing support of cloud free line of sight determination, including whole sky imaging of clouds, final report for ONR contract N00014-01-D-0043 DO #13," Marine Physical Laboratory, Scripps Institution of Oceanography, University of California, San Diego, ADA474969 (2007).
47. D. R. E. Brown, "Natural illumination charts," Report 374-1, Project Ns-714-100, Department of the Navy, Bureau of Ships, Washington, DC (1952).
48. K. YA. Kondrat'yev, "Actinometry," NASA TT F-9712, Translation of "Aktinometriya," Gidrometeorologicheskoye Izdatel'stvo, Leningrad (1965).
49. B. W. Hapke, "A theoretical function for the lunar surface," J. Geophys. Res. **68**, 4571–4585 (1963).
50. E. D. Hoffleit and W. H. Warren, Jr., *The Bright Star Catalogue*, 5th ed. (Astronomical Data Center and Yale University Observatory, 1991).
51. R. W. Johnson, M. E. Karr, and J. R. Varah, "Automated visibility measurements with a solid-state imager," University of California, San Diego, Scripps Institution of Oceanography, Marine Physical Laboratory, SIO Ref. 91-34, PL-TR-91-2016, ADA246892 (1990).
52. J. E. Shields, R. W. Johnson, and M. E. Karr, "An automated observing system for passive evaluation of cloud cover and visibility," University of California, San Diego, Scripps Institution of Oceanography, Marine Physical Laboratory, SIO 92-22, PL-TR-2202, NTIS No. ADA263207 (1992).
53. J. E. Shields, R. W. Johnson, M. E. Karr, A. R. Burden, and J. G. Baker, "Calibrated fisheye imaging systems for determination of cloud top radiances from a UAV," Proc. SPIE **5151**, 32–43 (2003).
54. J. E. Shields, J. G. Baker, M. E. Karr, R. W. Johnson, and A. R. Burden, "Visibility measurement along extended paths over the ocean surface," Proc. SPIE **5891**, 58910L (2005).
55. J. E. Shields, R. W. Johnson, J. G. Baker, M. E. Karr, and A. R. Burden, "Multispectral scattering measurements along extended paths using an imaging system," Proc. SPIE **6303**, 63030E (2006).
56. R. W. Johnson, "Method and apparatus for viewing target," U.S. patent 7,327,513 (5 February 2008).
57. M. C. Allmen and W. P. Kegelmeyer, Jr., "The computation of cloud base height from paired whole sky imaging cameras," Sandia Report SAND-94-8223 (Sandia National Laboratories, 1994).
58. G. Seiz, J. E. Shields, U. Feister, E. P. Baltsavias, and A. Gruen, "Cloud mapping with ground-based photogrammetric cameras," Int. J. Remote Sens. **28**, 2001–2032 (2007).
59. A. Cazorla, J. E. Shields, M. E. Karr, F. J. Olmo, A. R. Burden, and L. Alados-Arboledas, "Technical note: determination of aerosol optical properties by a calibrated sky imager," Atmos. Chem. Phys. **9**, 6417–6427 (2009).